RESEARCH ARTICLE

Figures and figure supplements

Negative feedback couples Hippo pathway activation with Kibra degradation independent of Yorkie-mediated transcription

Sherzod A Tokamov *et al*

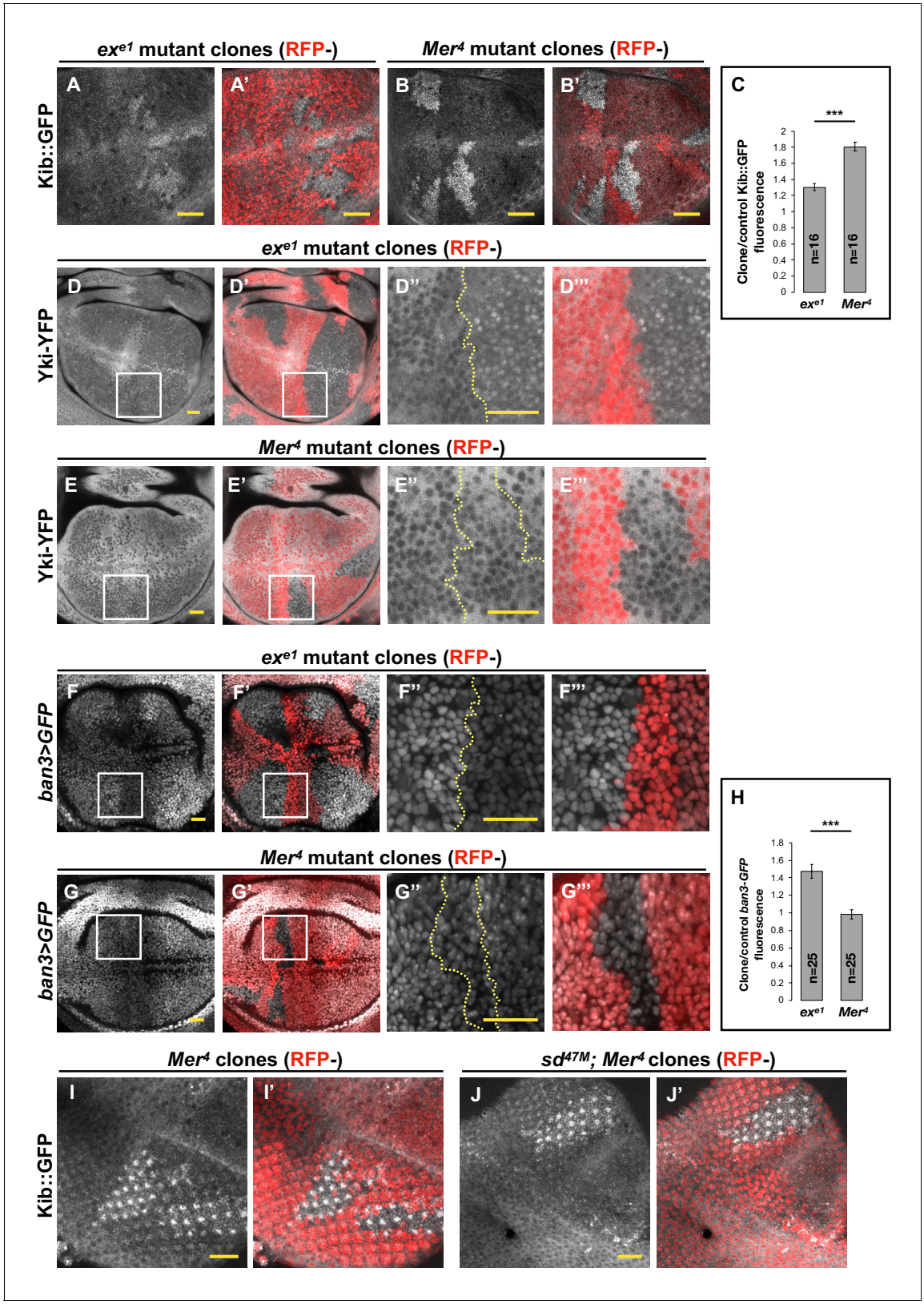

Figure 1. Transcriptional feedback alone does not explain Kibra (Kib) upregulation in *Mer* clones. (**A–G'''**) All tissues shown are living late third instar wing imaginal discs expressing the indicated fluorescent proteins. (**A–C**) Endogenous Kib::GFP in *ex* (**A and A'**) or *Mer* (**B and B'**) somatic mosaic clones (indicated by loss of RFP). Loss of Mer leads to a greater increase in Kib levels than loss of Ex. Quantification is shown in (**C**). (**D–E'''**) Endogenously

Figure 1 continued on next page

Figure 1 continued

expressed Yorkie (Yki)-YFP is strongly nuclear in *ex* mutant clones (**D–D'''**) but is mostly cytoplasmic in *Mer* mutant clones (**E–E'''**). (**F–H**) Expression *ban3>GFP*, a reporter of Yki activity, is elevated in *ex* mutant clones (**F–F'''**) but is not detectably affected in *Mer* mutant clones (**G–G'''**). Quantification is shown in (**H**). (**I–J'**) Endogenous Kib:GFP levels are elevated in single *Mer* somatic mosaic clones (**I and I'**) and in double *sd; Mer* clones (**J and J'**). Yellow dashed lines indicate clone boundaries. All scale bars=20 μm. Quantification in (**C**) and (**H**) is represented as the mean ± standard error of the mean (SEM); n=number of clones (no more than two clones per wing disc were used for quantification). Statistical analysis was performed using nonparametric Mann–Whitney U-test. Throughout the paper, statistical significance is reported as follows: ***$p \leq 0.001$, **$p \leq 0.01$, *$p \leq 0.05$, ns (not significant, $p > 0.05$).

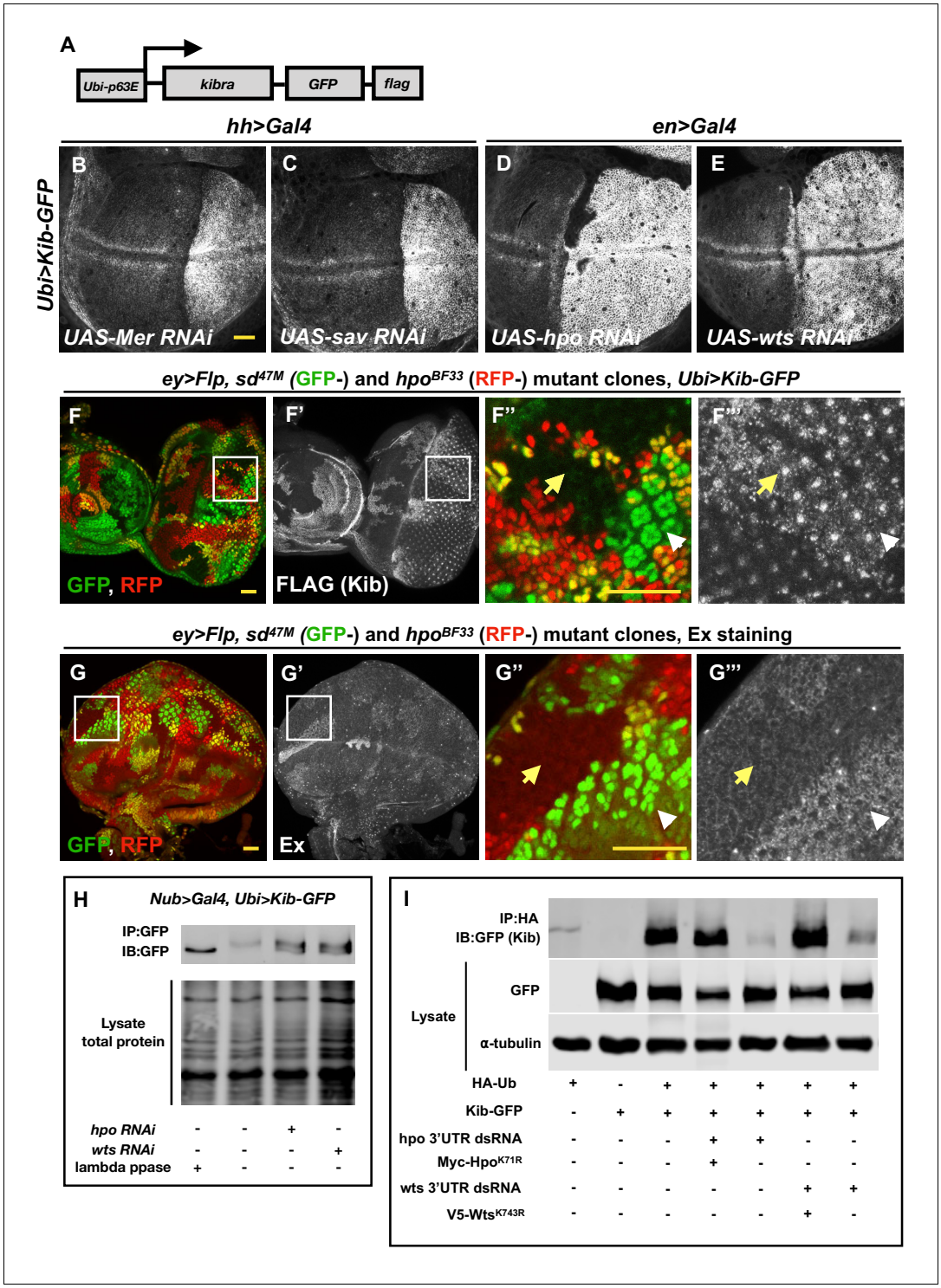

Figure 2. The Hippo (Hpo) pathway regulates Kibra (Kib) levels independently of Yorkie (Yki)-mediated transcription. (**A**) A cartoon of the DNA construct used to generate the *Ubi>Kib-GFP* transgenic fly line. (**B–E**) Depletion of Hpo pathway components Mer, Sav, Hpo, and Wts by RNAi in the posterior compartment of the wing results in elevated Kib-GFP levels. All scale bars=20 µm. Throughout the paper, wing imaginal discs are oriented with posterior side to the right and dorsal side up. (**F–F'''**) In the eye imaginal disc, Kib-GFP is upregulated both in *hpo* mutant clones and *sd; hpo* double-mutant clones, indicating that Hpo pathway activity controls Kib levels independently of Yki/Sd-mediated transcription. White arrowheads indicate *hpo* single-mutant clones; yellow arrows indicate *sd; hpo* double-mutant clones. Note: the clonal GFP marker (sd^{+}), which is nuclear,

Figure 2 continued on next page

Figure 2 continued

is readily distinguishable from Kib-GFP, which is apical. (**G–G'''**) Ex levels are also upregulated in *hpo* mutant clones; but in contrast to Kib, Ex upregulation is not observed in *sd; hpo* double-mutant clones. (**H**) Kib is phosphorylated in wing discs, and depletion of Hpo or Wts leads to decreased Kib phosphorylation. (**I**) Kib is ubiquitinated in S2 cells. Depletion of Hpo or Wts with dsRNA targeting 3'-untranslated region (UTR) of each kinase leads to decreased Kib ubiquitination; the effect of Hpo or Wts knockdown is rescued by addition of kinase-dead Hpo^{K71R} or Wts^{K743R}. Throughout the paper, all immunoblot data are representative of at least three replicates.

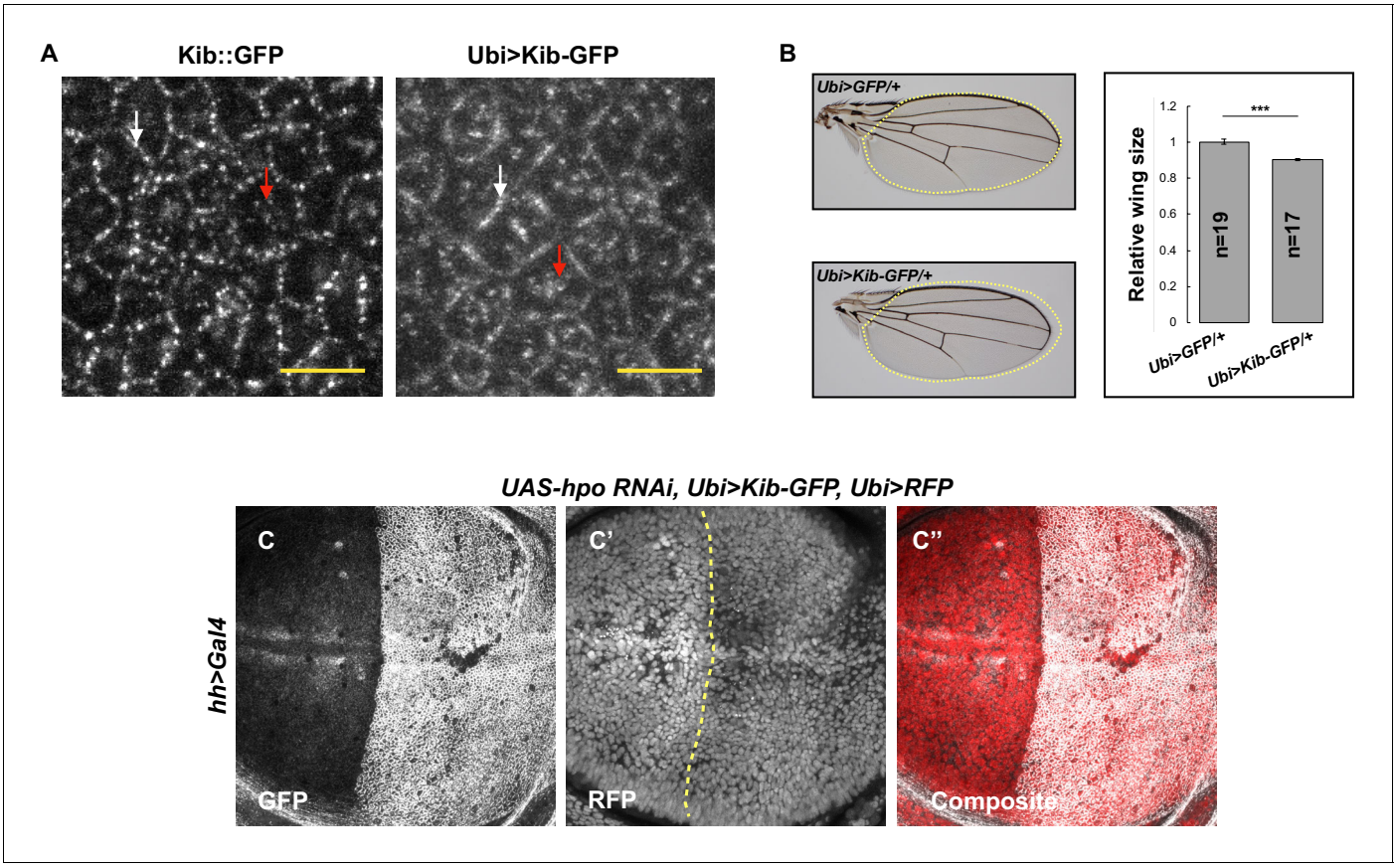

Figure 2—figure supplement 1. The Hippo pathway regulates Kibra (Kib) levels independently of Yorkie (Yki) transcriptional activity. (**A**) Similar to endogenous Kib:GFP (left), Ubi>Kib-GFP (right) accumulates both at the junctional (white arrows) and apical medial cortex (red arrows). Scale bars=5 µm. (**B**) Size comparison of adult wings from flies expressing *Ubi>GFP* or *Ubi>Kib-GFP*; quantification is shown as the mean ± SEM relative to the control; n=number of wings. Statistical comparison was performed using Mann–Whitney *U*-test. (**C–C''**) Depletion of Hpo in the posterior compartment of the wing does not cause increased Ubi>RFP expression. Yellow dashed line indicates the anterior–posterior (A–P) boundary.

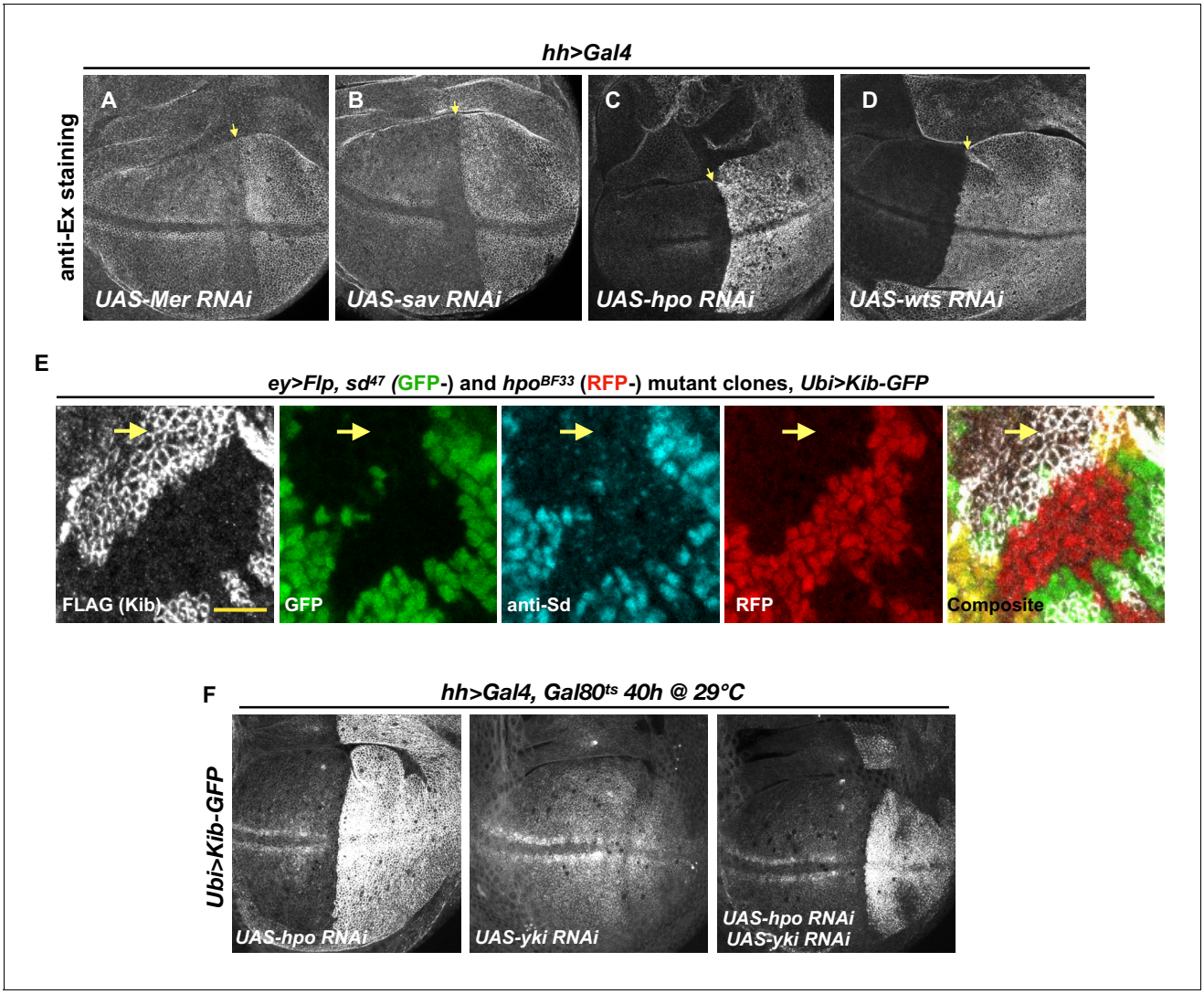

Figure 2—figure supplement 2. The Hippo (Hpo) pathway regulates Kibra (Kib) levels independently of Ex. (**A–D**) Ex levels are elevated upon Hpo pathway inactivation, with a particularly strong increase upon Hpo or Wts depletion (**C** and **D**, respectively). (**E**) Single *sd* (GFP-) or *hpo* (RFP-) somatic mosaic clones or double *sd; hpo* clones (GFP- and RFP-, yellow arrow) induced in the eye imaginal disc using *ey>Flp*. Ubi>Kib-GFP (FLAG staining) is upregulated in *sd; hpo* double-mutant clones; loss of *sd* was confirmed by anti-Sd staining (cyan). Scale bars=10 μm. (**F**) Effect of transient depletion of Hpo (left), Yki(middle), or Hpo and Yki (right) on Ubi>Kib-GFP levels in the posterior compartment of the wing using Gal80^{ts}.

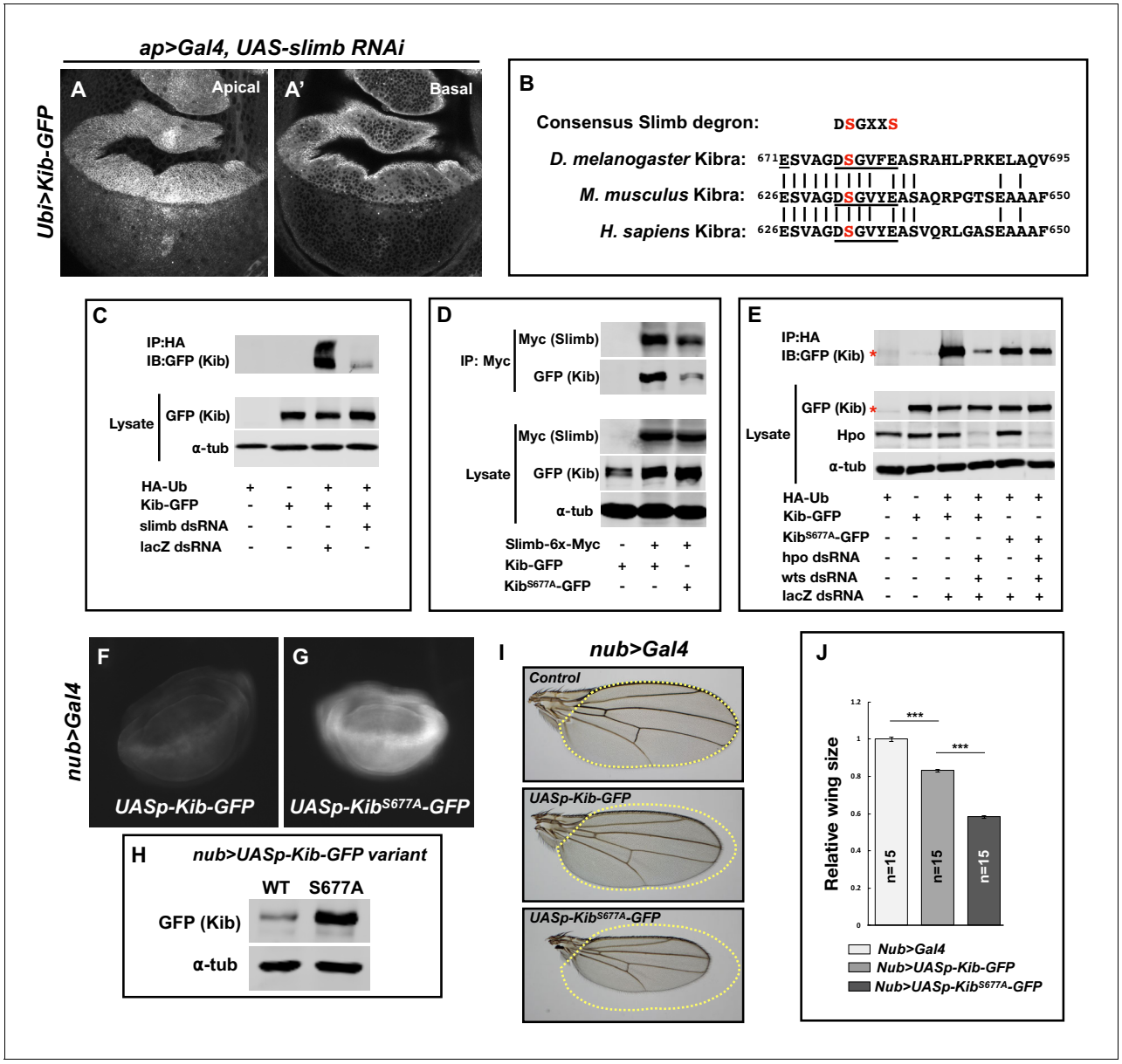

Figure 3. Slimb regulates Kibra (Kib) abundance via a consensus degron. (**A–A'**) Depletion of Slimb in the dorsal compartment of the wing imaginal disc results in increased Kib-GFP levels both apically (**A**) and basally (**A'**). (**B**) Alignment of the fly, mouse, and human Kib protein sequences showing the conservation of the putative Slimb degron motif DSGXXS (underlined). The vertical lines indicate conserved residues. (**C**) Immunoblot showing that depletion of Slimb in S2 cells decreases Kib ubiquitination. (**D**) Co-IP experiments showing that Kib forms a complex with Slimb in S2 cell lysates in a degron-dependent manner. (**E**) Ubiquitination of the degron mutant, Kib^{S677A}, is diminished and is insensitive to Hippo pathway inactivation. Asterisks indicate non-specific bands. (**F–G**) Widefield fluorescence images of wing discs expressing either *UASp-Kib-GFP* (**F**) or *UASp-Kib^{S677A}-GFP* (**G**) with the *nub>Gal4* driver; images were taken using identical settings. (**H**) Immunoblot of wing disc cell lysates (20 discs each) of *UASp-Kib-GFP* or *UASp-Kib^{S677A}-GFP* expressed with the *nub>Gal4* driver. (**I–J**) Ectopic expression of Kib^{S677A}-GFP in the wing results in stronger growth suppression than expression of wild-type Kib-GFP. Quantification of wing sizes in (**I**) is represented as mean ± SEM relative to the control; n=number of wings (one wing per fly). Statistical comparison was performed using the one-way analysis of variance (ANOVA) test followed by Tukey's Honestly Significant Difference (HSD) test.

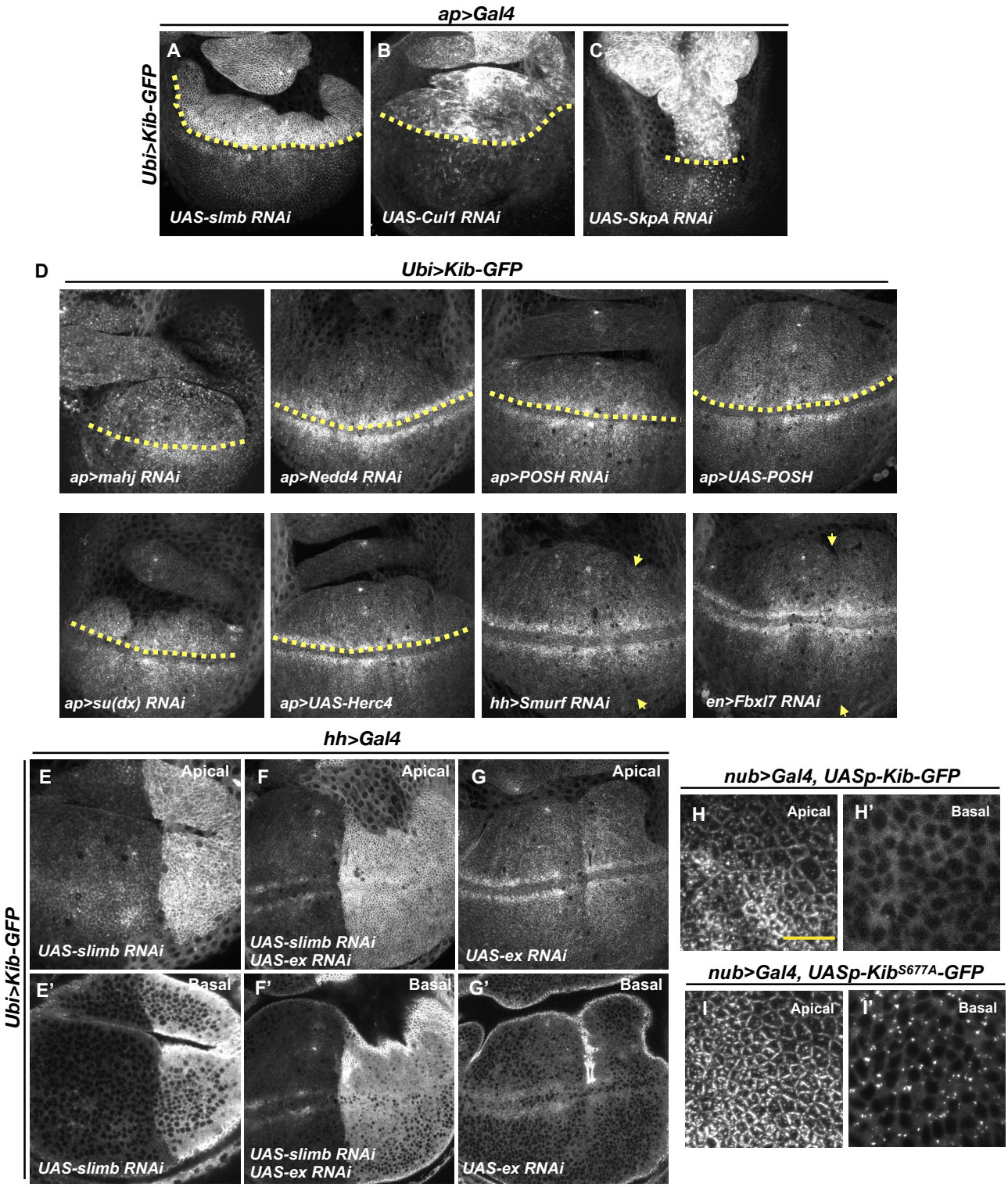

Figure 3—figure supplement 1. Effect of different E3 ubiquitin ligases involved in the Hippo (Hpo) pathway on Kibra (Kib) levels. (**A–C**) Depletion of SCF^{Slimb} E3 ubiquitin ligase components Slimb (**A**), Cul1 (**B**), or SkpA (**C**) in the dorsal compartment of the wing imaginal disc results in increased Ubi>Kib-GFP levels. (**D**) Depletion or overexpression of other E3 ubiquitin ligases known to regulate Hpo pathway components has no effect on Ubi>Kib-GFP levels. Yellow dashed line represents the dorsal–ventral boundary, with dorsal side up (for ap>Gal4); yellow arrows indicate the anterior–

Figure 3—figure supplement 1 continued on next page

Figure 3—figure supplement 1 continued

posterior boundary, with posterior to the right (for hh and en>Gal4). (**E–G′**) Ubi>Kib-GFP levels are elevated upon depletion of Slimb alone or co-depletion of Slimb and Expanded (Ex), but not when Ex alone is depleted in the posterior compartment of the wing imaginal disc. (**H–I′**) Confocal images of Kib-GFP or Kib^{S677A}-GFP expressed under UASp control with nub>Gal4. Kib^{S677A}-GFP shows similar localization to Kib-GFP apically but Kib^{S677A}-GFP forms foci basally. Note that images in (**I**) and (**I′**) were taken at lower gain than images in (**H**) and (**H′**) to avoid saturation. Scale bars=10 μm.

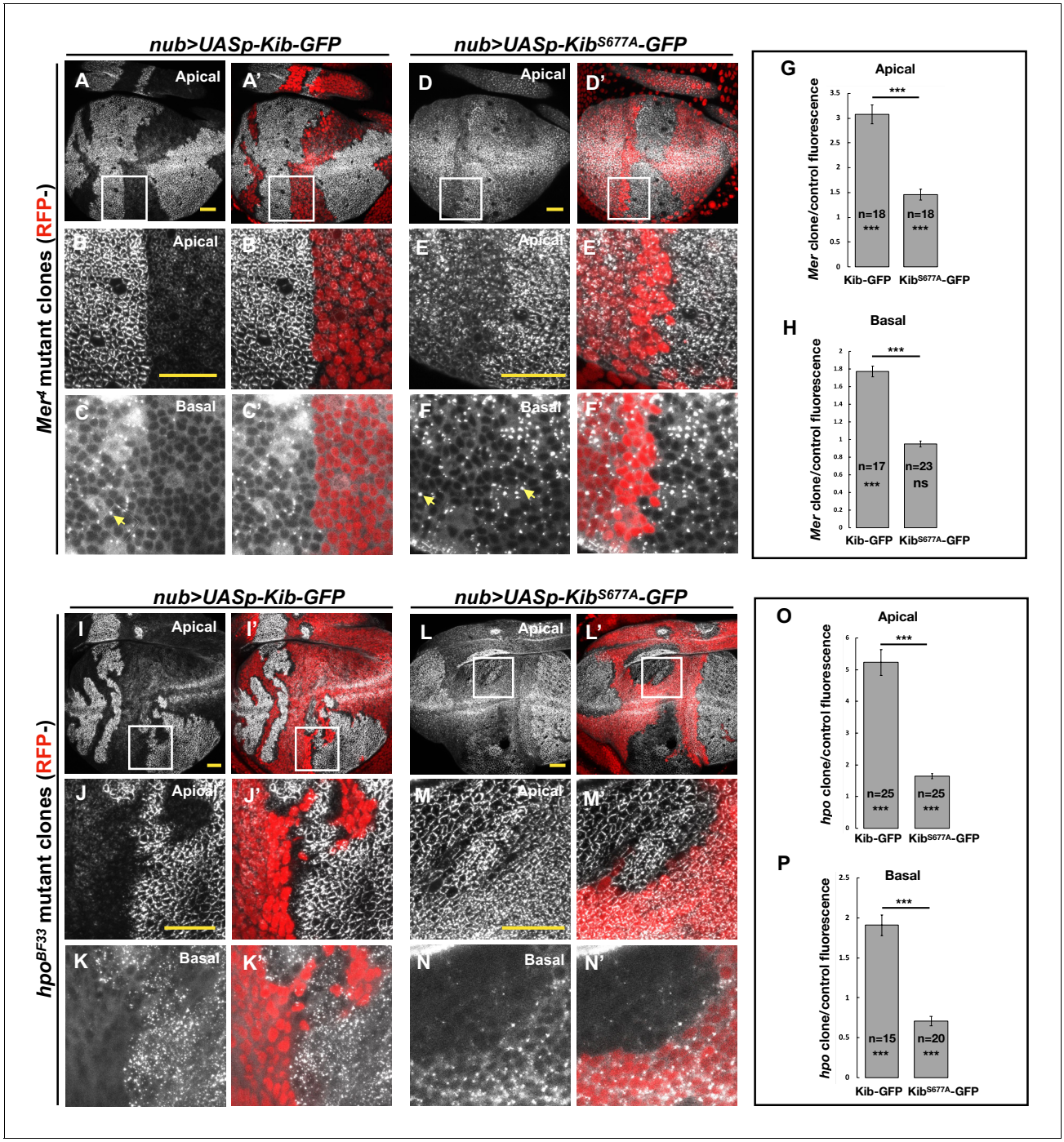

Figure 4. The Hippo pathway regulates Kibra (Kib) abundance via a putative degron motif. (**A–F'**) *Mer* somatic mosaic clones in wing discs expressing either *UASp-Kib-GFP* (**A-C'**) or *UASp-Kib^{S677A}-GFP* (**D–F'**) with the *nub>Gal4* driver. Note that wild-type Kib-GFP is significantly elevated in *Mer* clones both apically and basally, while Kib^{S677A}-GFP is only slightly stabilized apically and is not affected basally. Yellow arrows in C and F point to presumed Kib aggregates due to increased abundance. All scale bars=20 µm. (**G–H**) Quantification of clone/control ratio of apical (**G**) and basal (**H**) Kib-GFP fluorescence. All quantification is represented as the mean ± SEM; asterisks above the plots show p-values between the transgenes; asterisks inside each bar show p-values for each transgene with respect to 1; n=number of clones (no more than two clones per wing disc were used for quantification). Statistical comparison was performed using Mann–Whitney *U*-test. (**I–N'**) *hpo* somatic mosaic clones in wing discs expressing either *UASp-Kib-GFP* (**I–K'**) or *UASp-Kib^{S677A}-GFP* (**L–N'**) with the *nub>Gal4* driver. Note that wild-type Kib-GFP levels are significantly elevated in *hpo* clones both apically and basally, while Kib^{S677A}-GFP is stabilized apically but depleted basally in *hpo* clones. (**O–P**) Quantification of clone/control ratio of apical (**O**) and basal (**P**) Kib-GFP fluorescence.

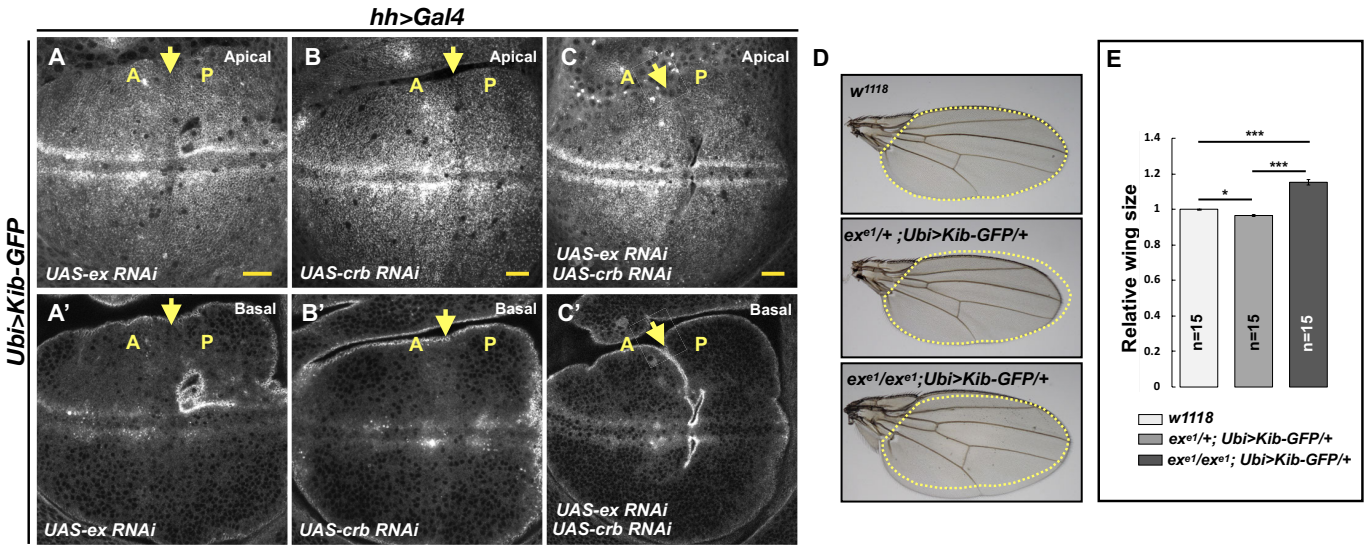

Figure 5. Kibra (Kib) abundance is regulated independently of Ex. (**A–C'**) Depletion of Ex (**A** and **A'**), Crumbs (Crb; **B** and **B'**), or both Ex and Crb (**C** and **C'**) in the posterior wing imaginal disc does not affect Ubi>Kib-GFP abundance. Yellow arrows indicate the anterior–posterior (A–P) boundary. Scale bars=20 µm. (**D–E**) Adult wings of w^{1118}, ex^{e1}/+; *Ubi>Kib-GFP/+*, or ex^{e1}/ex^{e1}; *Ubi>Kib-GFP/+* flies. Quantification of wing sizes in (**E**) is represented as the mean ± SEM; n=number of wings (one wing per fly). Statistical comparison was performed using the one-way ANOVA test followed by Tukey's HSD test.

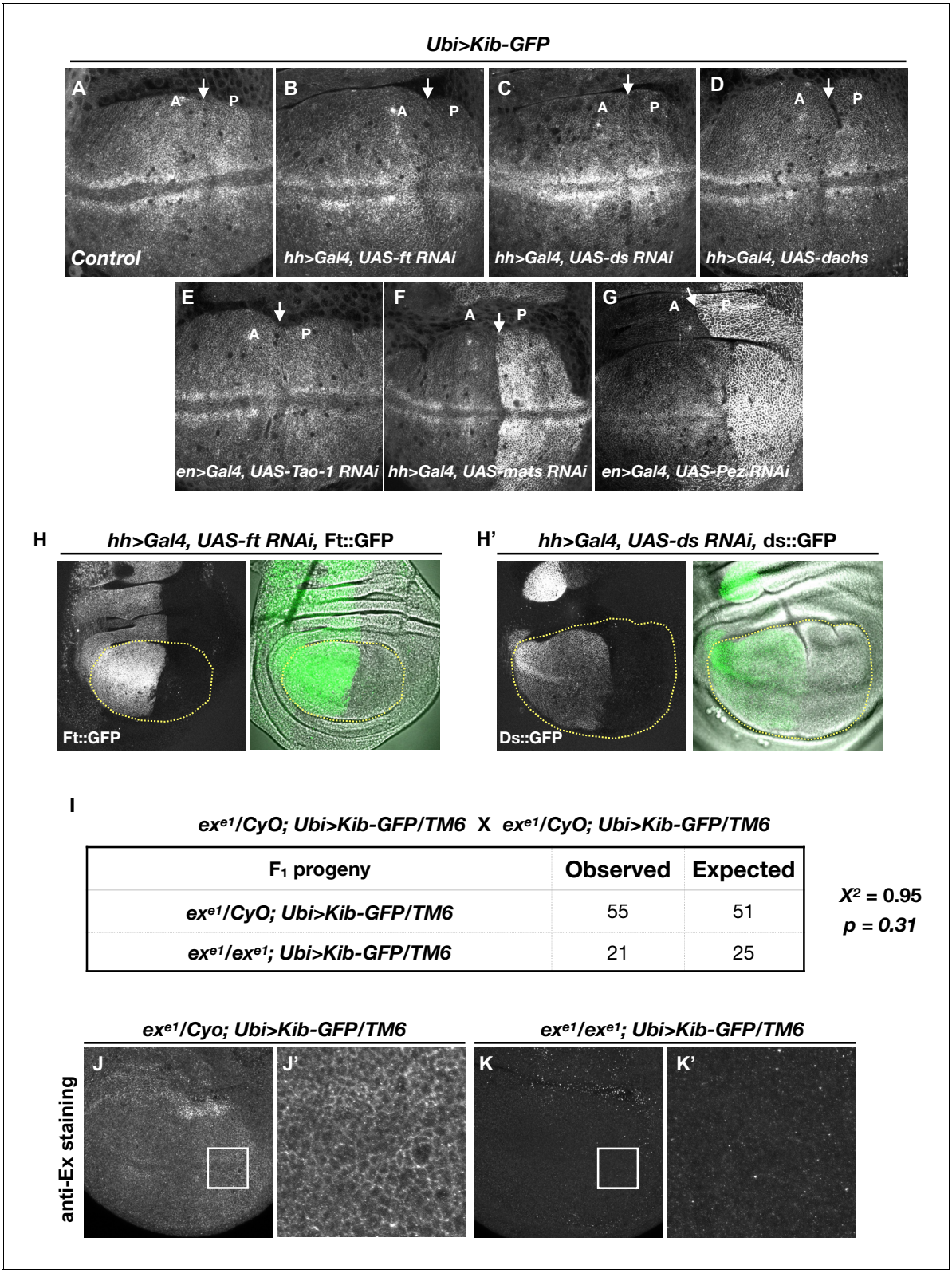

F1 progeny	Observed	Expected
ex^{e1}/CyO; Ubi>Kib-GFP/TM6	55	51
ex^{e1}/*ex*^{e1}; Ubi>Kib-GFP/TM6	21	25

Figure 5—figure supplement 1. The Hippo (Hpo) pathway controls Kibra (Kib) abundance in a tightly compartmentalized manner. (**A–G**) Kib abundance is regulated only by a subset of Hpo pathway components. (**H–H'**) Validation of RNAi lines against *ft* (**H**) and *ds* (**H'**) used to deplete these components in (**B**) and (**C**), respectively. (**I**) Chi-square analysis shows that *ex*^{e1} homozygotes survive as expected if ectopic Kib completely suppresses *ex* lethality. (**J–K'**) Ectopic Kib suppresses *ex*^{e1} lethality. Wing discs of *ex*^{e1} heterozygous larvae (**J** and **J'**) or *ex*^{e1} homozygous larvae (**K** and **K'**) carrying *Ubi>Kib-GFP* were stained for ExEx to confirm the presence of the *ex*^{e1} allele.

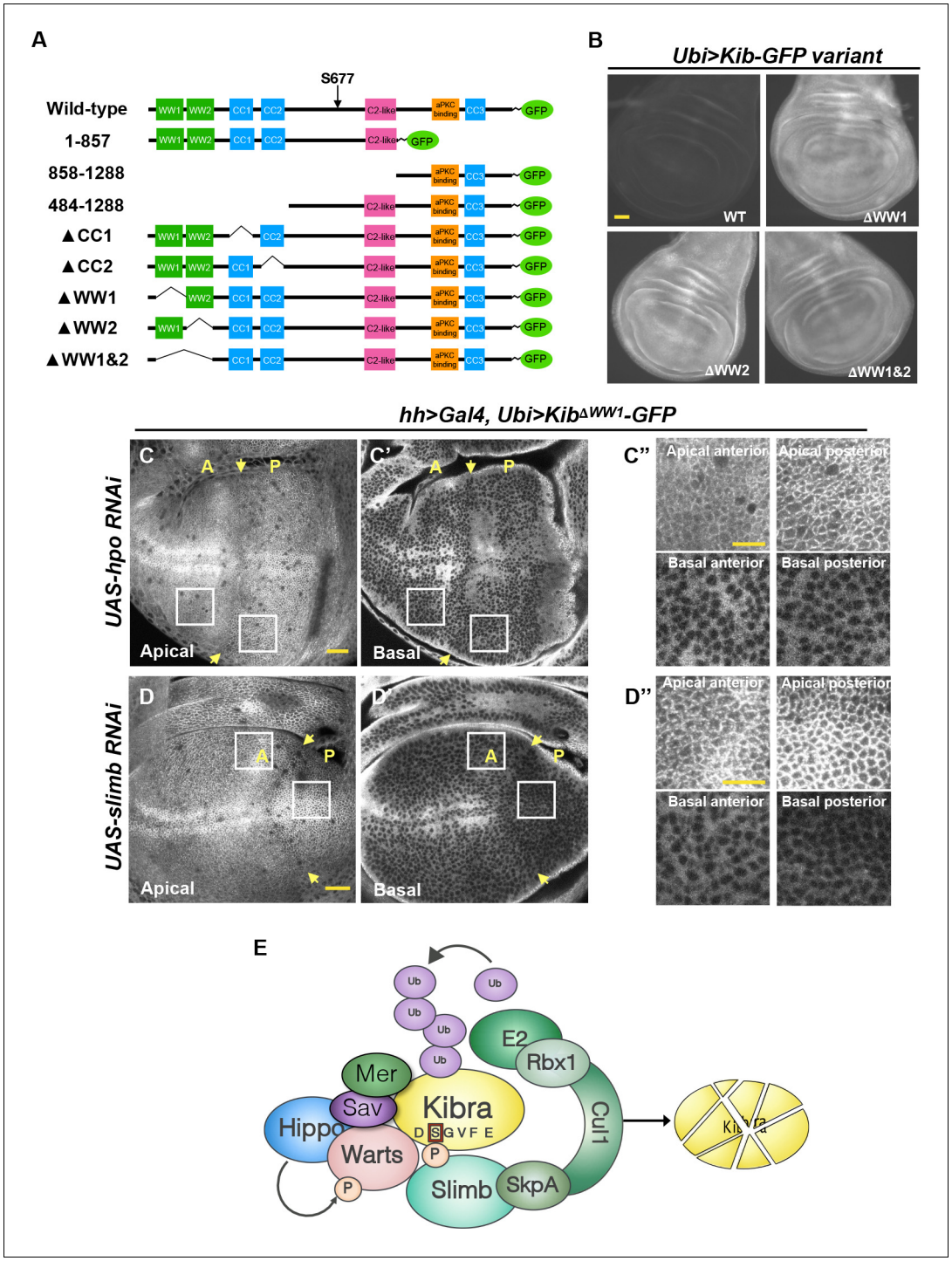

Figure 6. The WW domains of Kibra (Kib) are required for Hippo (Hpo) pathway- and Slimb-mediated degradation. (**A**) Diagram of Kib truncations generated for this study. (**B**) Widefield fluorescence images of wing imaginal discs expressing wild-type and WW-domain truncations of Kib-GFP expressed under the ubiquitin promoter. All images were taken with identical settings. Scale bar=40 μm. (**C–C''**) Depletion of Hpo does not affect expression of *Ubi>Kib*$^{\Delta WW1}$*-GFP*. Note that Hpo depletion leads to apical stabilization and basal depletion of Kib$^{\Delta WW1}$-GFP (**C''**). (**D–D''**) Depletion of Slimb does not affect expression of *Ubi>Kib*$^{\Delta WW1}$*-GFP*. Note that similar to Hpo depletion, loss of Slimb leads to slight apical stabilization and basal depletion of Kib$^{\Delta WW1}$-GFP (**D''**). Yellow arrows indicate A–P boundary of the wing discs. Scale bars=20 μm (**C and D**) and 10 μm (**C'' and D''**). (**E**) A model of Kib degradation by the Hpo pathway and Slimb.

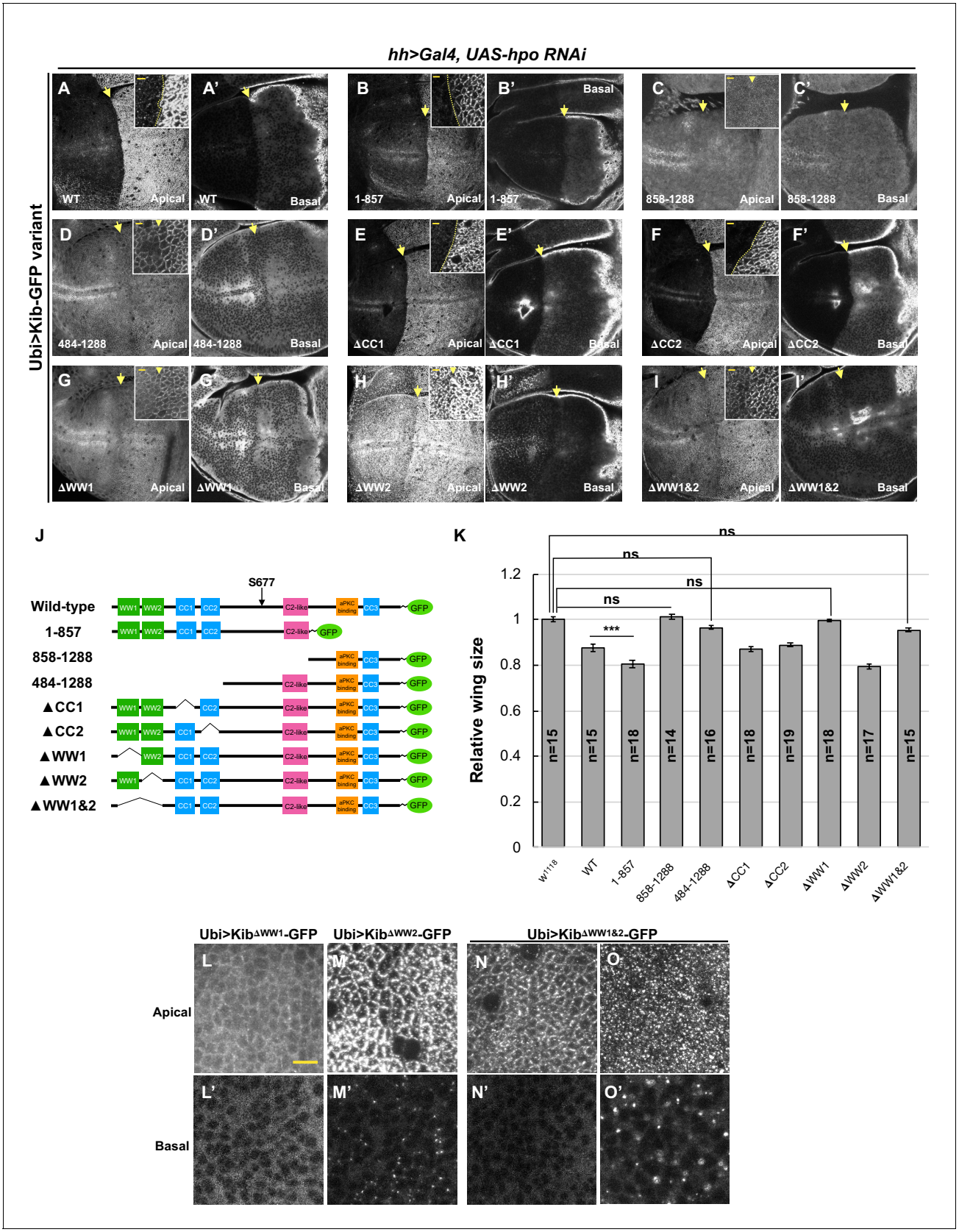

Figure 6—figure supplement 1. The role of WW domains in Hippo pathway-mediated Kibra (Kib) degradation. (**A–I'**) Effect of Hpo depletion in the posterior compartment of the wing imaginal disc on different Kib truncations. Deletion of the WW domains, individually (**G–H'**) or together (**I** and **I'**)

Figure 6—figure supplement 1 continued on next page

Figure 6—figure supplement 1 continued

stabilizes Kib apically but does not lead to an increase in basal Kib levels. Note that tissue in (**G**) is the same as shown in ***Figure 6C***. Scale bars in the insets represent 3 μm for the insets and 10 μm for the corresponding low magnification image. (**J**) Diagram of Kib truncations generated for this study (same as in ***Figure 6A***). (**K**) Size comparison (relative to wild-type) of adult wings from flies ectopically expressing different Ubi>Kib-GFP truncations. Quantification is shown as the mean ± SEM; n=number of wings. Statistical comparison was performed using the one-way ANOVA test followed by Tukey's HSD test. (**L–O'**) Localization of Kib lacking WW1 (**L** and **L'**), WW2 (**M** and **M'**), or both WW1 and WW2 (**N–O'**) in wing imaginal disc cells. Note that Ubi>Kib$^{\Delta WW1\&2}$-GFP localization is variable; sometimes it localizes normally at the junctions (**N**) and is diffused basally (**N'**), but usually it accumulates in bright foci both apically and basally (**O and O'**). Scale bar=10 μm.

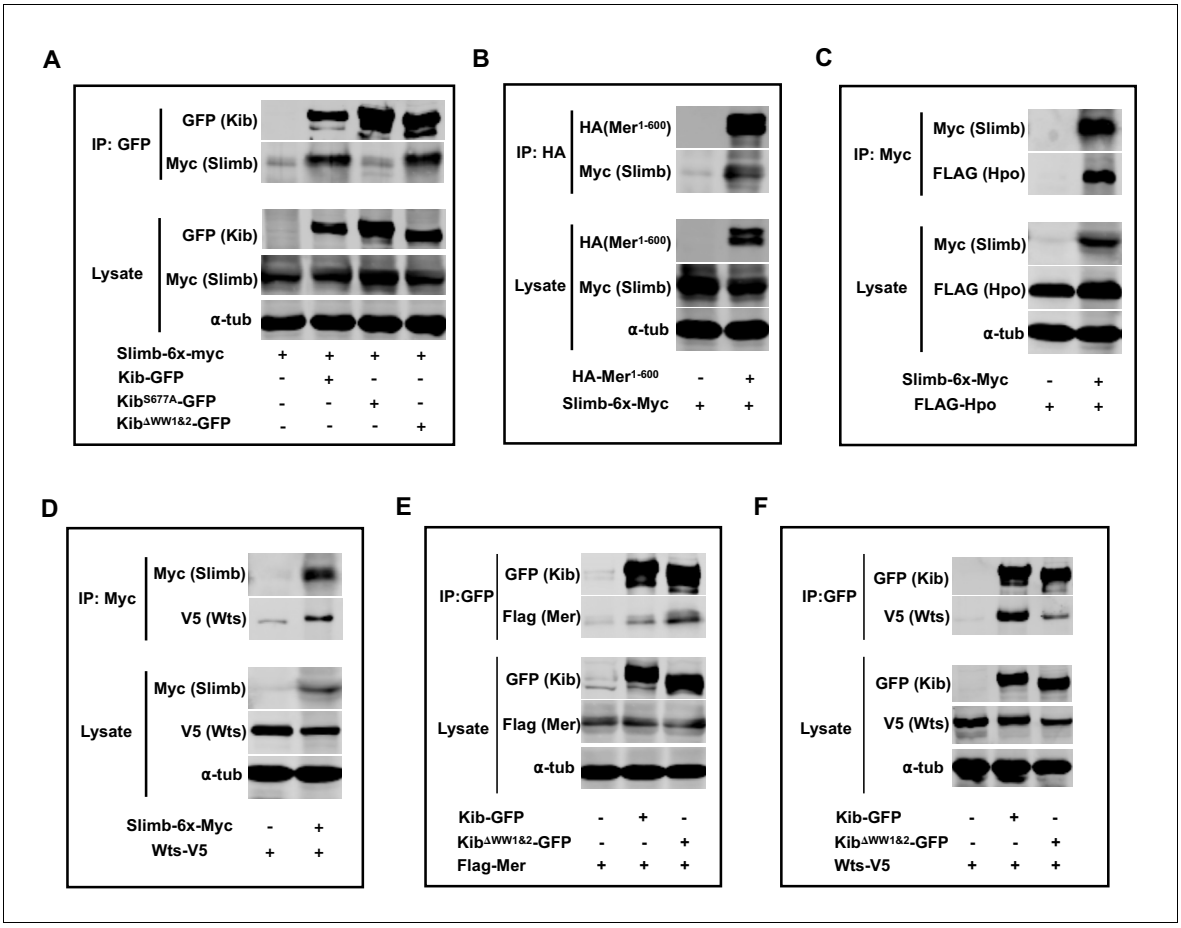

Figure 6—figure supplement 2. Complex formation and Kibra (Kib) degradation. (**A–D**) Slimb forms a complex with wild-type Kib and Kib$^{\Delta WW1\&2}$ (**A**), Mer$^{1-600}$ (**B**), Hpo (**C**), and Wts (**D**). (**E–F**) Co-IP of wild-type Kib or Kib$^{\Delta WW1\&2}$ with Mer (**E**) or Wts (**F**). All experiments were performed using lysates from transfected S2 cells.

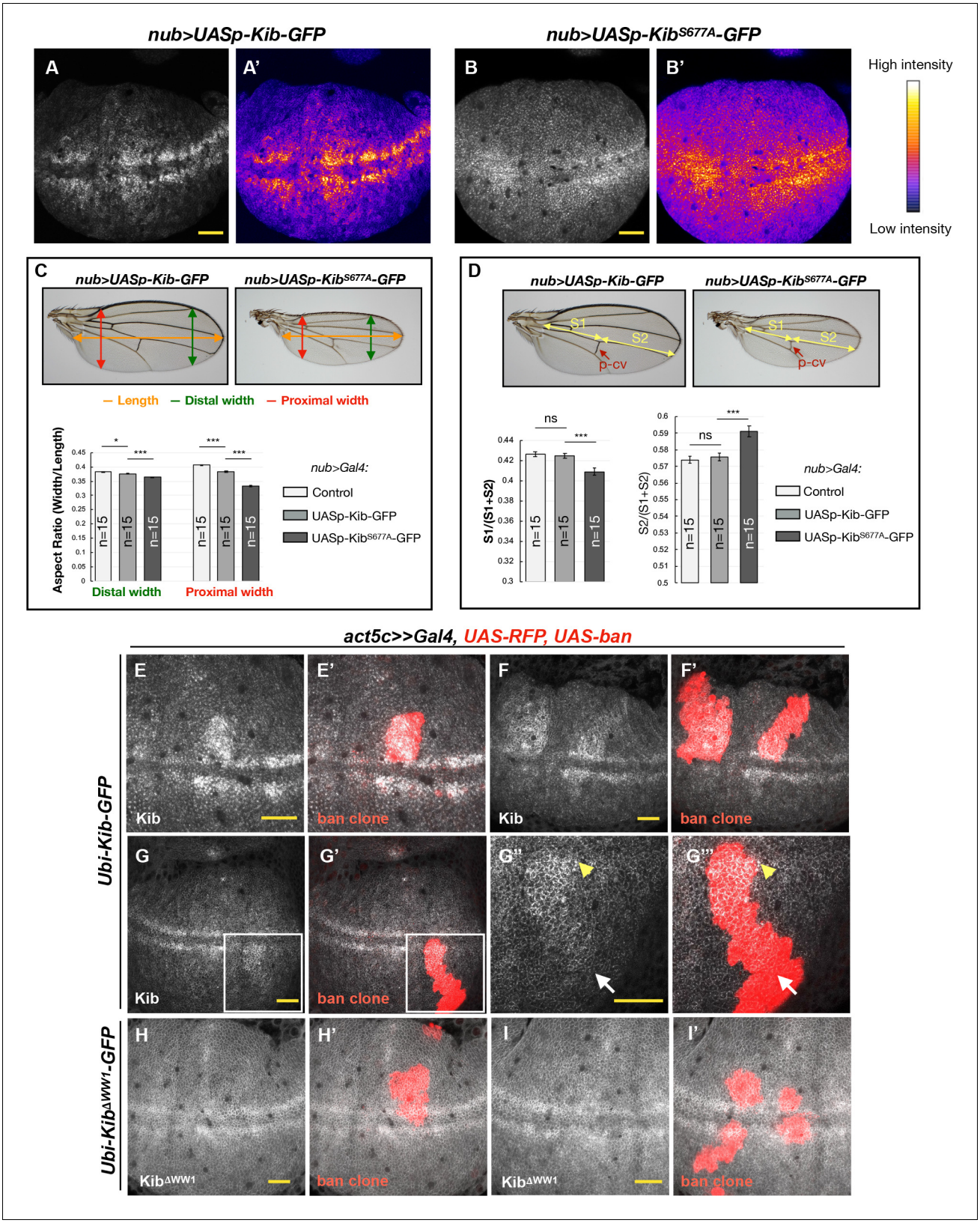

Figure 7. Kibra (Kib) degradation is patterned by mechanical tension in the wing pouch to control proportional growth. (**A–B'**) Grayscale images of the wing pouch, which produces the adult wing blade, expressing *UASp-Kib-GFP* (**A**) or *UASp-Kib*^{S677A}*-GFP* (**B**) at identical genomic locations under the *nub>Gal4* driver. Corresponding heatmap intensity images are shown in (**A'**) and (**B'**). Note that Kib^{S677A}-GFP displays a more uniform distribution

Figure 7 continued on next page

Figure 7 continued

across the pouch than wild-type Kib-GFP. (**C**) Quantification of aspect ratios of adult wings expressing *nub>Gal4* alone or with *UASp-Kib-GFP* and *UASp-Kib*^{S677A}*-GFP*. The color-coded segments in the wing image represent the wing length (orange), distal width (green), and proximal width (red). (**D**) Quantification of the length of proximal (**S1**) or distal (**S2**) wing region with respect to total wing length in wings expressing *nub>Gal4* alone or with *UASp-Kib-GFP* and *UASp-Kib*^{S677A}*-GFP*; p-cv=posterior crossvein. All quantification is represented as the mean ± SEM; n=number of wings (one wing per fly). Statistical comparison was performed using the one-way ANOVA test followed by Tukey's HSD test. (**E–F'**) Kib-GFP levels are elevated in rapidly proliferating *UAS-bantam* clones. (**G–G'''**) Increased Kib abundance is more pronounced at the center of the wing pouch (yellow arrowhead) than at its periphery (white arrow). (**H–I'**) Kib$^{\Delta WW1}$-GFP levels do not change in *bantam*-expressing clones. All scale bars=20 μm.

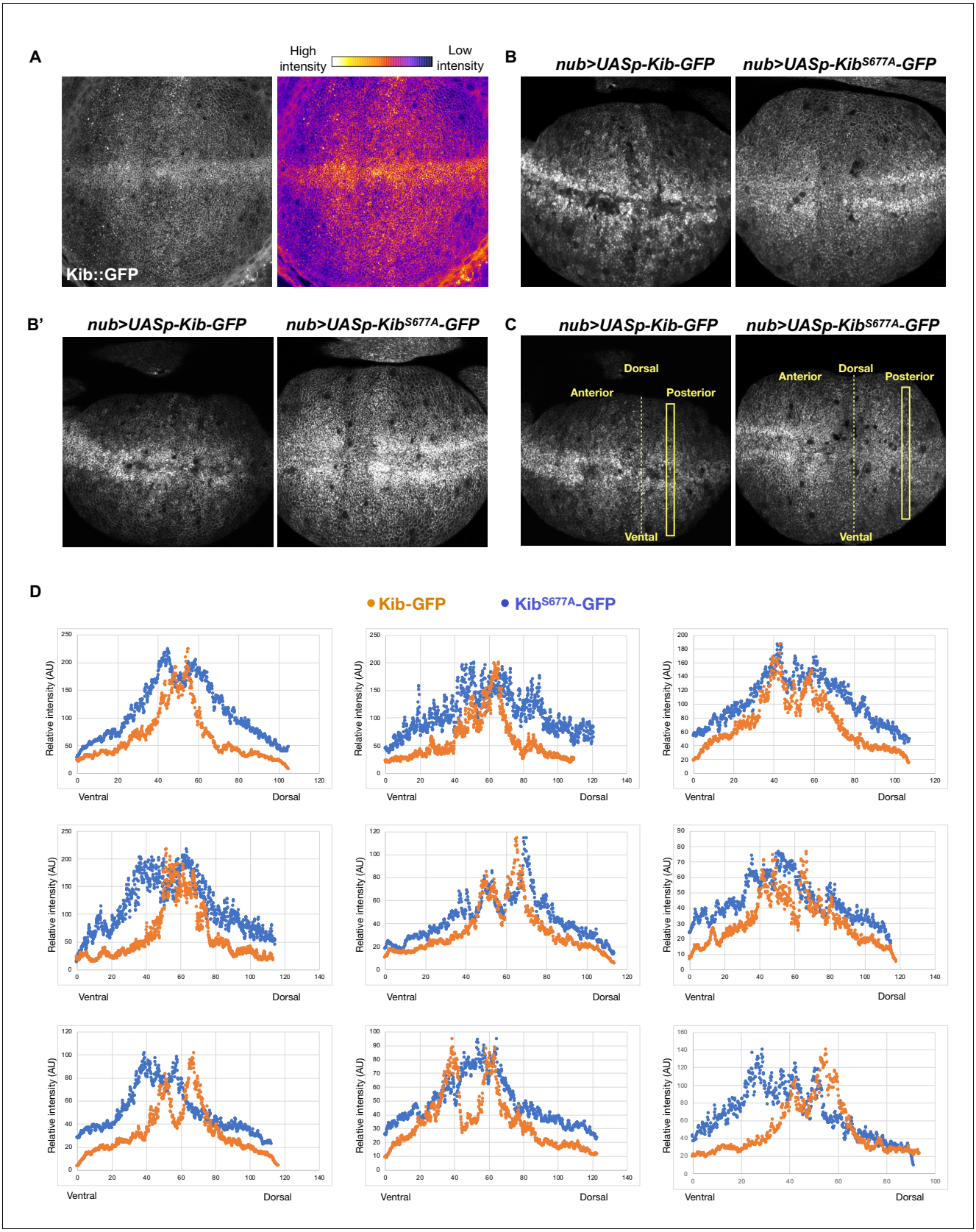

Figure 7—figure supplement 1. Kibra (Kib) degradation is not uniform across the pouch region of the wing imaginal disc. (**A**) A grayscale and heatmap image of a wing imaginal disc expressing endogenous Kib::GFP. (**B–B'**) Additional examples of wing discs expressing Kib-GFP or Kib^{S677A}-

Figure 7—figure supplement 1 continued on next page

Figure 7—figure supplement 1 continued

GFP under UASp control using the *nub>Gal4* driver focused on the wing pouch, which produces the adult wing blade. (**C**) To generate the intensity profiles in (**C**), rectangular selections of equal length were drawn on each disc either in the anterior or posterior region (same side was used for each pair). Intensity values from *UASp-Kib-GFP* discs were normalized to the maximum value of *UASp-Kib*^{S677A}*-GFP* discs. (**D**) Intensity profiles of nine pairs of wing imaginal discs expressing *UASp-Kib-GFP* or *UASp-Kib*^{S677A}*-GFP* under the *nub>Gal4* driver. In each case, wild-type Kib intensity drops more severely from the distal (middle) to proximal (most dorsal or ventral) part of the wing pouch.